Verifying Light Curves of Periodic Variable Stars Using Robotic Telescopes

Michael Anstett

24 April, 2020

Christopher Newport University

Adivsed by Dr. Gore

1 Abstract

This paper analyzes light curve data from five periodic variable stars. Apparent Magnitude data was taken from the variable stars designated as HIP 26295, 24500, 40853, 44847, and 54543. The stars were imaged using iTelescope from observatories in Mayhill, New Mexico and Conabarabran, Australia. The light curve was processed using the method of Fourier Decomposition. Raw data from the European Space Agency's Hipparcos project was used in this analysis to test the fit. Due to issues procuring data, this study was inconclusive.

2 Introduction

Periodic variable stars (frequently referred to as "pulsating") consistently vary in brightness over a repeating interval of time. The patterns of the change in brightness are documented in the from of "light curves," which plot magnitude, from brighter (lower numbers) to dimmer (higher numbers) as a function of the phase, taken as zero to one. For example, the light curve of HIP 26295 is listed in Figure 1. Periodic variable stars are categorized according to the shape of their light curves and the length of their period. The main categories of periodic variable stars are listed in Table 1 (1).

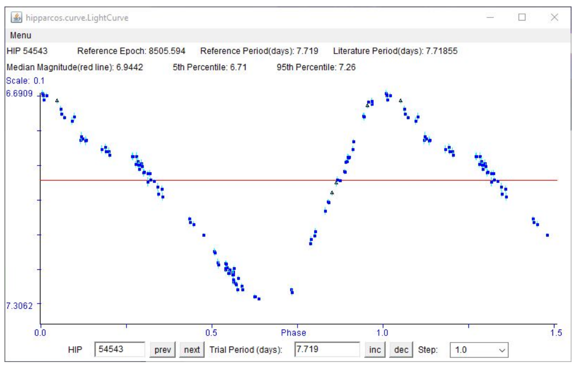

Figure 1: An Example Light Curve (2)

Table 1: Types of Variable Stars and their Period Range

Types	Period Range
Cepheids	1-135 days
Long-period variables	30-10,000 days
Mira	80-1,000 days
Semiregular	30-1,000 days
RR Lyrae	1.5 hours - 1 day

These stars vary due to intrinsic characteristics of the stars chemistry and structure. Many lie on a section of the Hertzsprung-Russell diagram referred to as the 'instability strip.' Cepheids and RR Lyrae in particular are very useful to astrometric study, as the length (as shown in Table 1) of their period is closely related to their absolute magnitude through the period-luminosity relationship. This allows one to determine their distance, which can be extrapolated to analysis of surrounding stars.

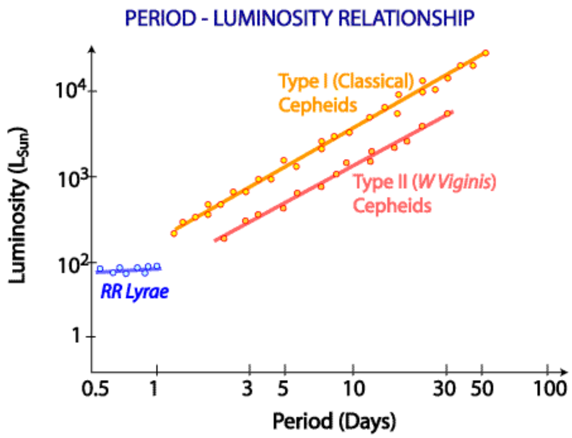

Figure 2: The Period-Luminosity Relationship (7)

Another form of periodic variable stars are eclipsing binaries. An eclipsing binary is a system of orbiting stars which regularly pass in front or behind each other from the perspective of the Earth. The masses of these stars are determined based on the time it takes for them to transit each other.

Aside from pulsating stars, cataclysmic variable stars can show dramatic magnitude changes over a short, non-repeating period. The magnitudes of these stars change as a consequence of large cataclysmic events such as supernova. The light curves of these stars do not repeat periodically, so new data cannot be compared to past data. Pulsating variables and eclipsing binaries will be the focus of this study, as the light curves of these stars can be compared to established light curves.

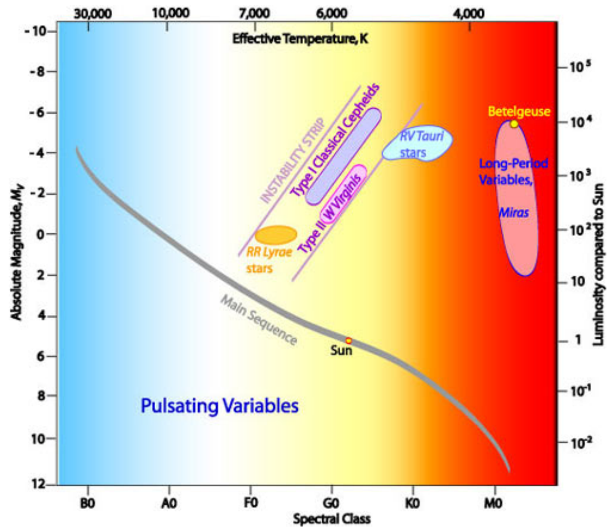

Figure 3: The range of pulsating variable stars on the Hertzsprung-Russel Diagram (6)

3 Theory

Each observation consisted of 2 captures of 120 seconds each. HIPs 26295 and 24500 were imaged using a visual light filter, and HIPS 40853, 44847, 54543 were imaged using a blue light filter, as T8 does not have a visual filter. For the purposes of comparison to data in the visual band, the B-V color index listed in the HIP catalogue was used. Magnitudes were computed using 'Vphot,' the American Association of Variable Star Observer's online photometry software. A reference star with a known, constant magnitude in each field was used to compute magnitudes. The reference star data can be found in Appendix 3. Raw data was plotted as magnitude, from dimmer to brighter, as a function of time elapsed in seconds.

As for producing a function based on the fitting of the light curve, the method of Fourier Decomposition was used. I used the method developed by Schlatenbrand and Tammann in 1971, which creates a function based on a fourier series expansion. The following equations define the expression of the Fourier series and coefficients (4) (5):

$$m(t) = A_o + \sum_{i=1}^{N} a_i \cos(2\pi\Phi(t)) + \sum_{i=1}^{N} b_i \sin(s\pi\Phi(t)), \tag{1}$$

$$\Phi = \frac{(t - t_o)}{P} - Int(\frac{t - t_o}{P}) \tag{2}$$

$$a_i = \frac{1}{N+1} \sum_{i=1}^{N} f(x_i) \cos(i\pi x_i) \tag{3}$$

$$b_i = \frac{1}{N+1} \sum_{i=1}^{N} f(x_i) \sin(i\pi x_i) \tag{4}$$

The evaluation of these formulas was made using a Mathematica notebook. Phase and magnitude data were imported from an Excel workbook and used to calculate the coefficients through a for loop. The series of a particular order N expansion was then calculated with another for loop. This analysis was done on data taken from the HIP archive and the data taken from iTelescope. In order to perform the preliminary analysis, the data from HIP 26295 was plotted as phase against magnitude as well.

4 Methods

Five stars were chosen for study in this paper. Of primary concern were the visibility of the stars over a long period of time for each location. Stars with celestial coordinates accessible by the observatories throughout the months selected for study were prioritized. The HIP catalogue, which numbers stars depending on their right ascension coordinates, was used to search for stars. Secondly, stars were selected having periods both short enough to be potentially measured several times through the study, and long enough so that observation over several nights was possible. Finally, star choices were made based on diversity of the types available. The table below lists the stars selected for study. The Hipparchos Project data for these stars can be found in Appendix 1.

Table 2: Target Information

HIP Number	RA (hh:mm:ss)	Dec (^{o},',")	Period (days)	Max V_{mag}	Min V_{mag}	B-V	Type	Alternative Classifications
26295	05:35:58.47	+24:44:54.3	6.73	9.96	11.03	0.696	Herbig Ae/Be	CQ Tau, HD 36910
24500	05:15:21.98	+40:04:40.9	18.20	10.02	10.90	1.540	Classical Cepheid	YZ Aur
40853	08:20:10.66	-23:21:33.4	3.82	7.77	8.28	-0.006	Eclipsing Binary	V434 Pup, HD 70258
44847	09:08:15.76	-51:26:10.7	6.92	7.61	8.04	1.120	Classical Cepheid	BG Vel, HD 78801
54543	11:09:41.15	-58:50:15.8	7.72	6.71	7.26	0.831	Classical Cepheid	ER Car, HD 97082

HIPs 26295 and 24500 were measured from telescope T5 at New Mexico Skies Observatory, located in Mayhill, New Mexico. HIPs 40853, 44847 and 54543 were measured from T8 at Siding Springs Observatory in Conabarabran, Australia. These telescopes are operated remotely through the iTelescope network through scripts (see Appendix 2 for an example) the observer provides. Below is a table of the information of the two observatories and telescopes

New Mexico Skies Observatory	
Coordinates	32.90N, 105.53W
Telescope T5	
Aperature	250mm
Focal Length	850mm (f/3.4)
Imager: SBIG Universal	
Detector Size	2184 by 1472p
FOV Size	59.99' $\times$ 40.43'
Plate Scale	1.65"/px $\times$ 1.65"/px
Filters	R, G, B, C, Halpha, SII, OIII, B, V, I

Siding Springs Observatory	
Coordinates	-31.27N, 149.07W
Telescope T8	
Aperature	106mm
Focal Length	530mm (f/5.0)
Imager: SBIG Universal	
Detector Size	4096 × 4096 px
FOV Size	238.80’ × 238.80’
Plate Scale	3.5”/px × 3.5”/px
Filters	Luminance, Red, Green, Blue, Exo, Hα, SII, OIII, I

5 Data

5.1 Raw Data from Vphot

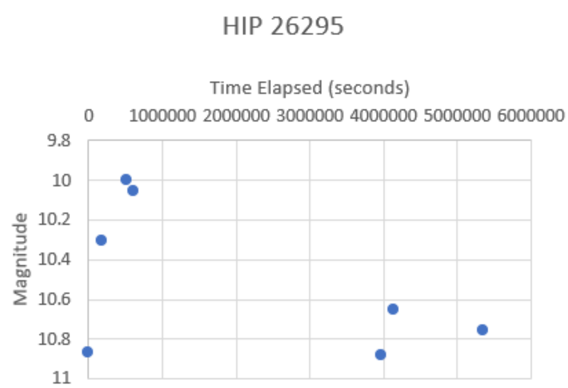

Figure 4: HIP 26295 Data from Vphot

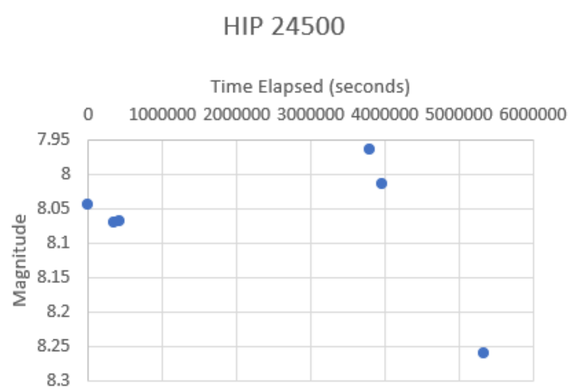

Figure 5: HIP 24500 Data from Vphot

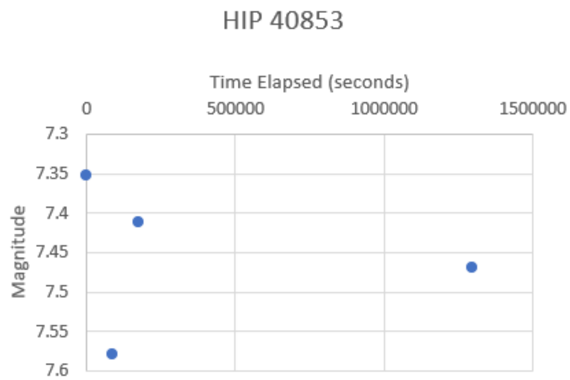

Figure 6: HIP 40853 Data from Vphot

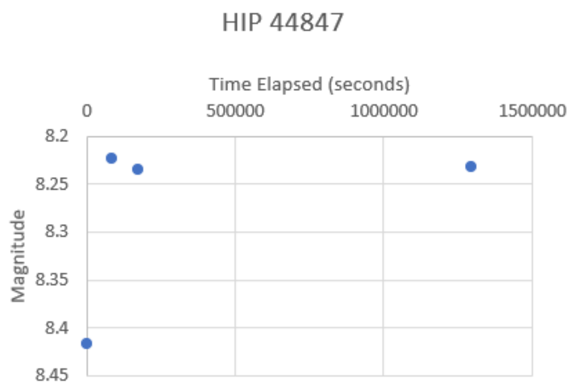

Figure 7: HIP 44847 Data from Vphot

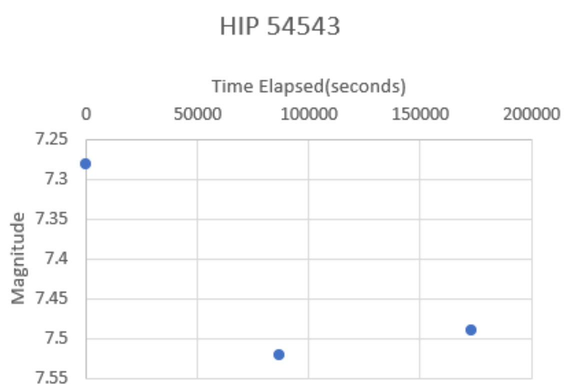

Figure 8: HIP 54543 Data from Vphot

5.2 Fourier Expanded Data

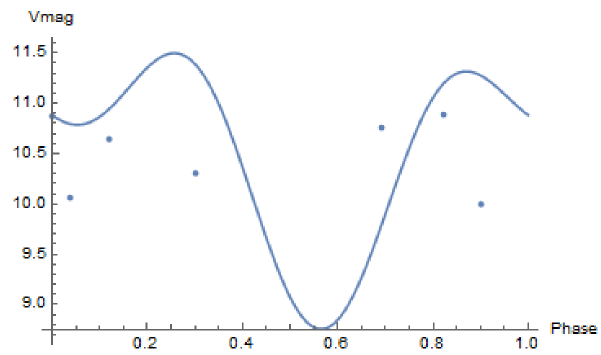

Figure 9: Fourier Expanded Data for HIP 26295, N=2

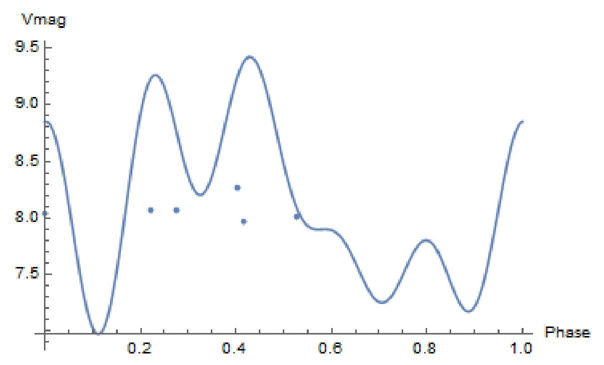

Figure 10: HIP 24500, N=2, N=2

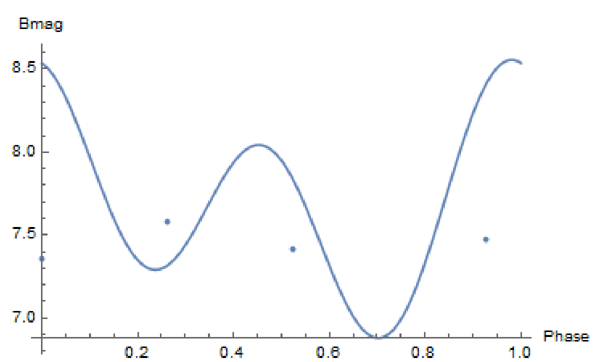

Figure 11: HIP 40853, N=2

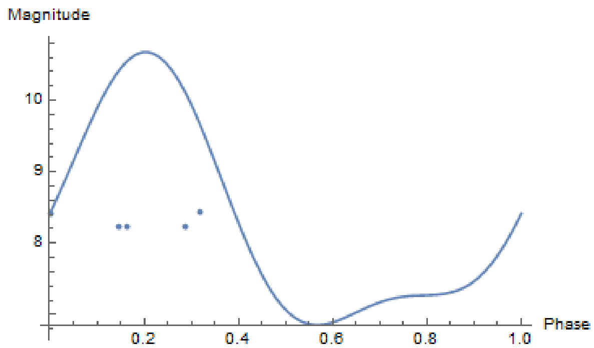

Figure 12: HIP 44847, N=2

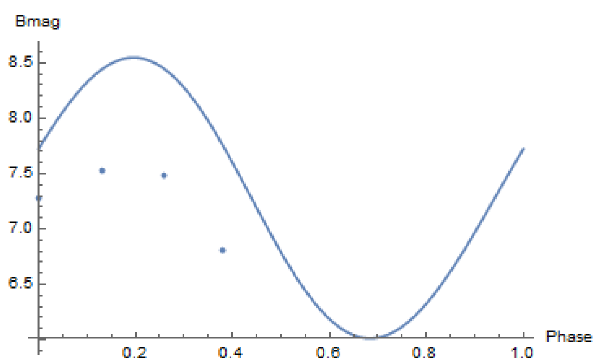

Figure 13: HIP 54543, N=2

5.3 HIP Archive Fourier Expanded Data

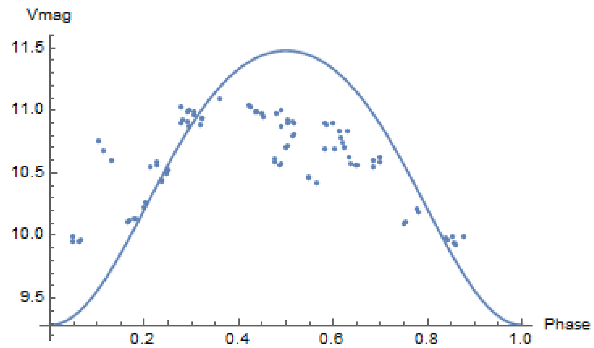

Figure 14: N=2 Fourier Expanded Data for HIP 26295

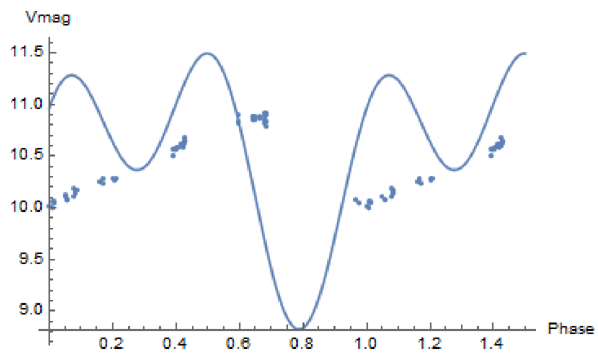

Figure 15: N=2 Fourier Expanded Data for HIP 26295

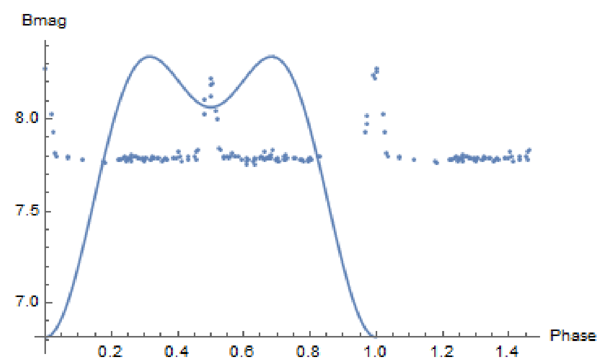

Figure 16: N=2 Fourier Expanded Data for HIP 26295

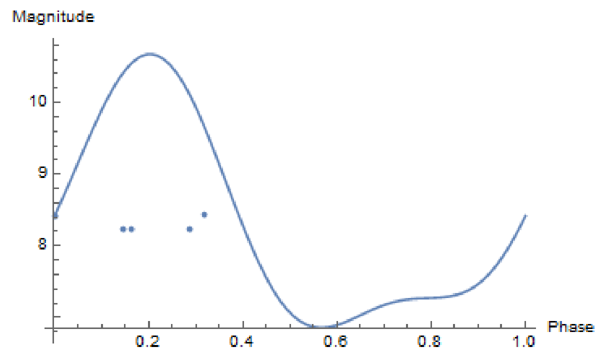

Figure 17: N=2 Fourier Expanded Data for HIP 26295

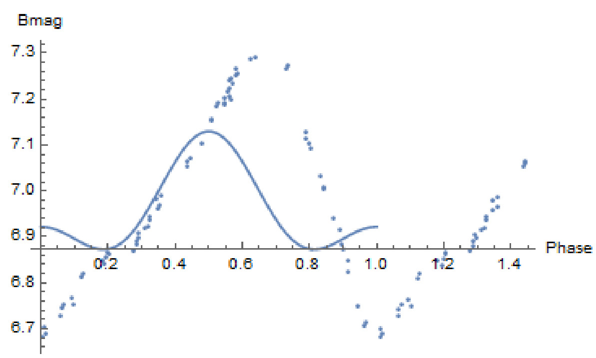

Figure 18: N=2 Fourier Expanded Data for HIP 26295

6 Discussion and Conclusions

The lack of data is the primary concern regarding this study's success. During the roughly three months of study, the majority of scheduled observations were cancelled or not scheduled due to the observatory roofs being closed, and even more were simply not scheduled due to the forecast. Towards the end of the observing period, traffic drastically increased on the iTelescope schedule. During this time, I also had to be more selective with the times at which I scheduled observations, as dayglow approached the targets. This further limited the capacity at which I could take data. If I were to do a similar observation-based project again, I would be more selective over the time at which I took data, as well as make sure to schedule runs far in advance of other users.

The Fourier decomposition method highlighted in this paper, by visual inspection, also does not fit the forms I had expected. Although apparently used in light curve characterization studies, it seems better equipped for more spread out data. Fourier decomposition expresses a set of points as a sum of the trigonometric functions with coefficients defined by the value of the point and its phase. Having multiple points around the same phase likely contributed to the amplified curve visible in the plots.

7 Appendices

7.1 Appendix 1 - Raw Data from HIP Archive

Taken from the Hipparcos light curve Java Applet.

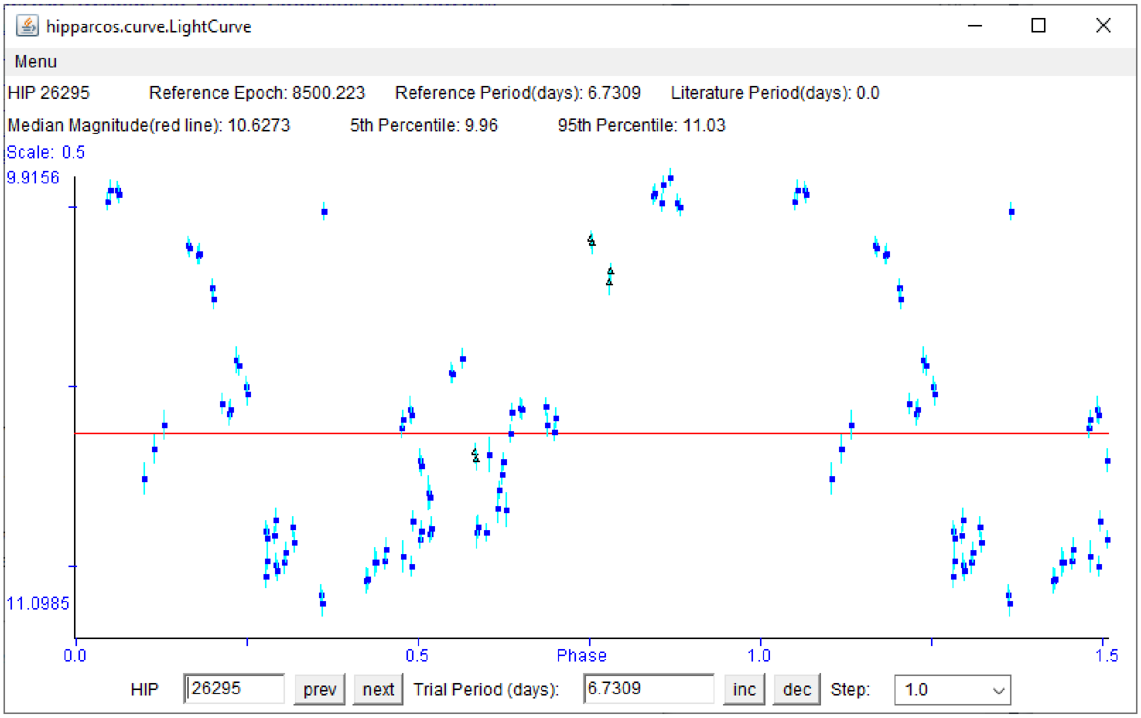

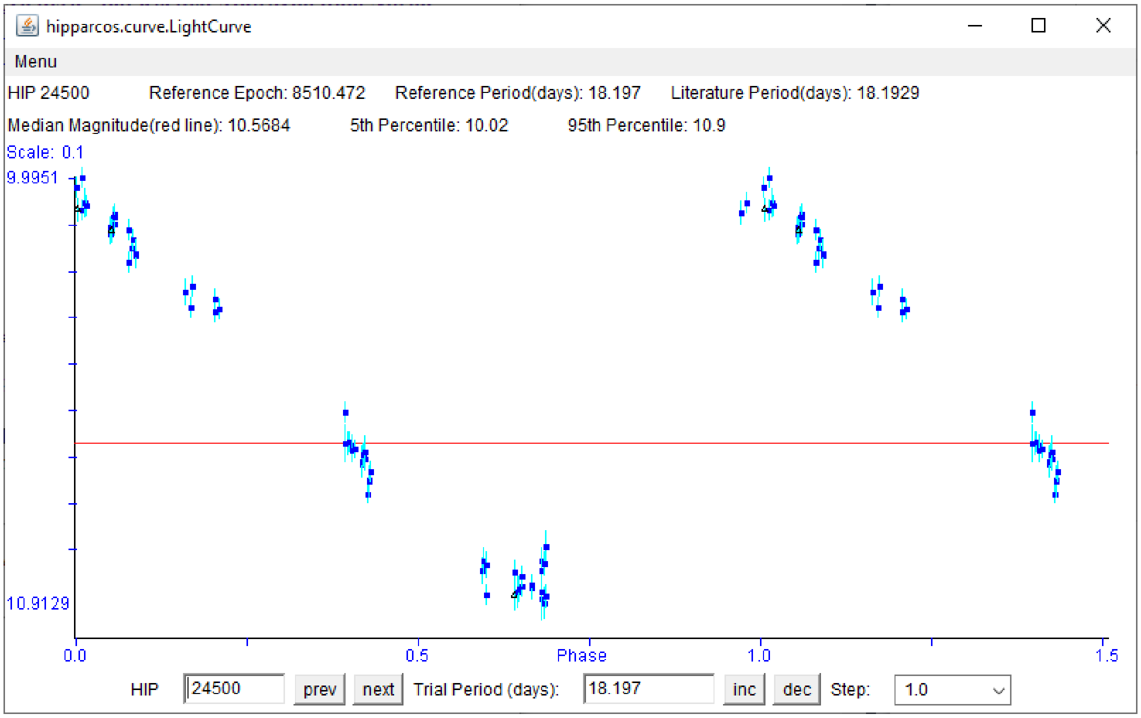
hipparcos.curve.LightCurve
Menu
HIP 24500 Reference Epoch: 8510.472 Reference Period(days): 18.197 Literature Period(days): 18.1929
Median Magnitude(red line): 10.5684 5th Percentile: 10.02 95th Percentile: 10.9
Scale: 0.1
9.9951
10.9129
0.0
0.5
Phase
1.0
1.5
HIP
24500
prev
next
Trial Period (days):
18.197
inc
dec
Step:
1.0

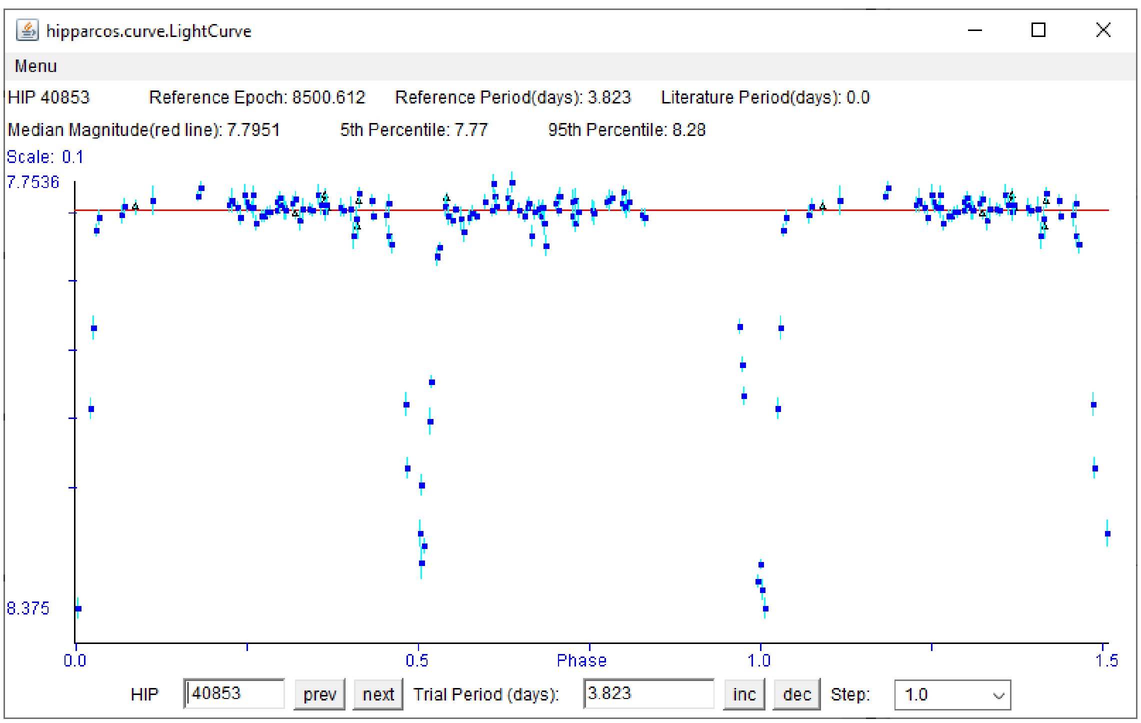
hipparcos.curve.LightCurve
Menu
HIP 40853 Reference Epoch: 8500.612 Reference Period(days): 3.823 Literature Period(days): 0.0
Median Magnitude(red line): 7.7951 5th Percentile: 7.77 95th Percentile: 8.28
Scale: 0.1
7.7536
8.375
0.0
0.5
Phase
1.0
1.5
HIP
40853
prev
next
Trial Period (days):
3.823
inc
dec
Step:
1.0

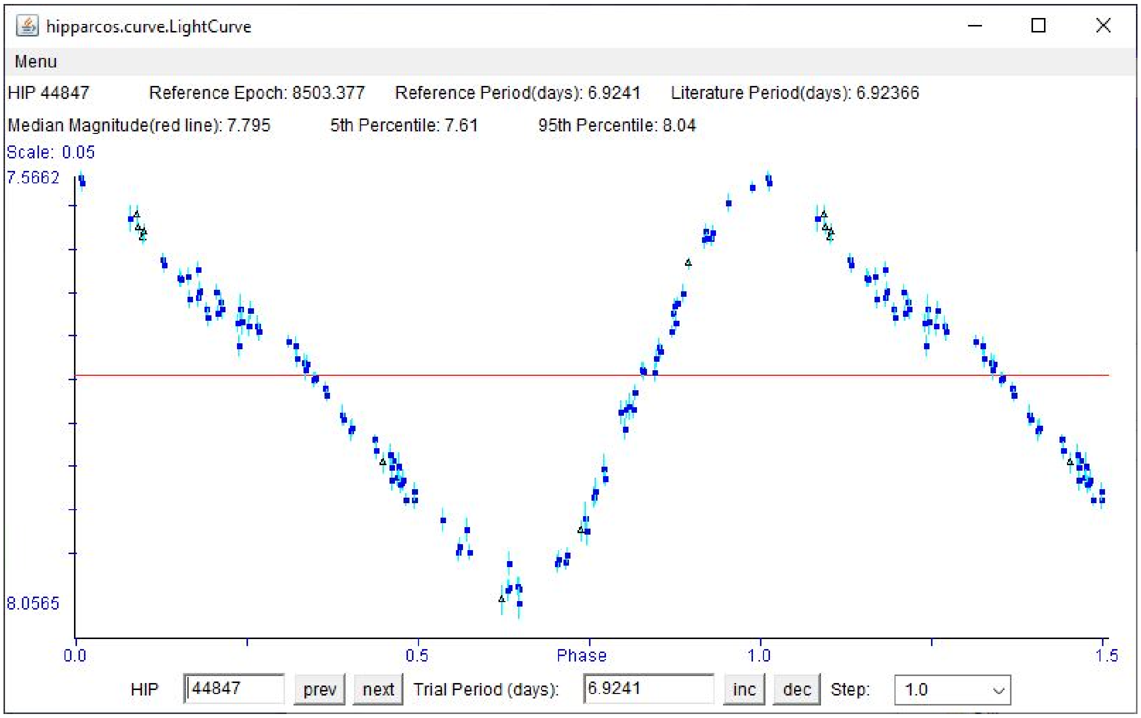
hipparcos.curve.LightCurve
Menu
HIP 44847 Reference Epoch: 8503.377 Reference Period(days): 6.9241 Literature Period(days): 6.92366
Median Magnitude(red line): 7.795 5th Percentile: 7.61 95th Percentile: 8.04
Scale: 0.05
7.5662
8.0565
0.0
0.5
Phase
1.0
1.5
HIP 44847 prev next Trial Period (days): 6.9241 inc dec Step: 1.0

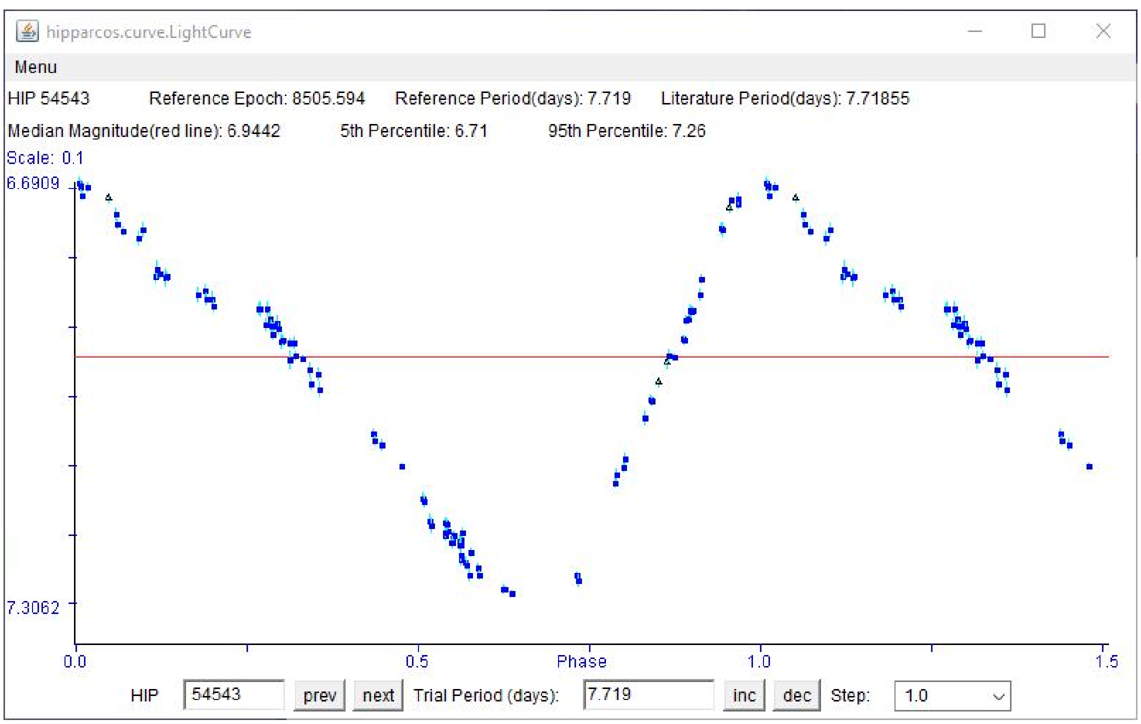
hipparcos.curve.LightCurve
Menu
HIP 54543 Reference Epoch: 8505.594 Reference Period(days): 7.719 Literature Period(days): 7.71855
Median Magnitude(red line): 6.9442 5th Percentile: 6.71 95th Percentile: 7.26
Scale: 0.1
6.6909
7.3062
0.0
0.5
Phase
1.0
1.5
HIP 54543 prev next Trial Period (days): 7.719 inc dec Step: 1.0

7.2 Appendix 2 - A Sample Script

#Filter V

#Count 2

#Interval 120

#Binning 2

HIP 26295 05:35:58.47 +24:44:54.3

#Chain HIP24500.txt

References

[1] Types of Variable Stars: A Guide for Beginners. (n.d.). Retrieved February 5, 2020.

[2] ESA, 1997, The Hipparcos and Tycho Catalogues, ESA SP-1200

[3] Deb, S., Singh, H. P. (2018). Light curve analysis of Variable stars using Fourier decomposition and Principal component analysis. Astronomy Astrophysics.

[4] Schaltenbrand, R., Tamman, G. A. (1971). The Light Curve Parameters of Photoelectrically Observed Galactic Cepheids. Astr. Astrophys. Suppl., 4, 265–314.

[5] Collins, G. W. (2003). Fundamental Numerical Methods and Data Analysis.

[6] CSIRO Australia Telescope National Facility, / Epping NSW. (2019, May 8). Types of Variable Stars.

[7] CSIRO Australia Telescope National Facility, Epping NSW. (2019, December 18). Cepheid Variable Stars Distance.